



Pergamon

Tetrahedron 57 (2001) 8543–8550

TETRAHEDRON

Intermolecular recognition between hydrocarbon oxygen-donors and perfluorocarbon iodine-acceptors: the shortest O···I non-covalent bond[☆]

Maria T. Messina,^a Pierangelo Metrangolo,^{a,*} Walter Panzeri,^b Tullio Pilati^c
and Giuseppe Resnati^{a,*}

^aDepartment of Chemistry, Polytechnic, 7 via Mancinelli, I-20131 Milan, Italy

^bC.N.R.—Centro Studio Sostanze Organiche Naturali, 7 via Mancinelli, I-20131 Milan, Italy

^cC.N.R.—Centro Studio Relazioni Struttura Reattività Chimica, University of Milan, 19 via Golgi, I-20133 Milan, Italy

Received 15 May 2001; revised 4 July 2001; accepted 26 July 2001

Abstract—Heteroaromatic *N*-oxides are shown to work as effective electron donors towards perfluorocarbon iodides. This non-covalent interaction is strong enough to drive the self-assembly of perfluorocarbon and hydrocarbon modules into discrete aggregates or one dimensional infinite networks and to give rise to the shortest O···I intermolecular distance reported to now in the crystallographic literature. The effectiveness of the O···I–R_F halogen bonding with respect to the better studied N···I–R_F interaction is discussed. © 2001 Elsevier Science Ltd. All rights reserved.

1. Introduction

The ability of hydrocarbon halides R_H–X (R_H=alkyl or aryl residue, X=I, Br, Cl) to work as electron-acceptor motifs (Lewis acids) and to give donor-acceptor complexes R_H–X···B (B=O, S, Se, N, ...) with a wide variety of neutral electron-donor motifs (Lewis bases) is well recognised² and it has been usefully employed in crystal engineering.³ This type of interaction has been rationalised as an n→σ* electron donation⁴ and has been called ‘halogen bonding’ to stress the similarity with the hydrogen bonding.¹

When perfluorocarbon (PFC) halides R_F–X (R_F=perfluoroalkyl or perfluoroaryl residue) are used as acidic motifs, and nitrogen substituted hydrocarbon (HC) compounds are employed as basic motifs, the interaction becomes strong^{5,31} enough to overcome the low affinity⁶ existing between PFC and HC derivatives and to drive the formation of PFC–HC supramolecular architectures.^{1,7} We have already shown how the R_F–I···N interaction pattern can involve structurally different iodo-PFCs (i.e. mono- and diiodoperfluoro-

alkanes and -arenes) and dinitrogen-HCs (i.e. secondary and tertiary aliphatic or aromatic amines, pyridine derivatives) invariably giving solid materials which are stable in air at room temperature. In order to generalise the use of the halogen bonding in the systematic and geometry-based design of PFC–HC supramolecular architectures, dibromoperfluoroarenes have been recently challenged with dinitrogen-HCs.^{3i,8} One-dimensional (1D) non-covalent co-polymers have been obtained in this case too, thus proving that also electron acceptor moieties different from iodine can effectively drive the PFC–HC self-assembly.

In this paper we describe some cases where HC modules the electron donor moiety of which is an oxygen atom can, not only effectively drive PFC–HC self-assembly processes, but they can be even more effective in the formation of the halogen bonded adducts than corresponding nitrogen substituted modules. For instance, the formation of the infinite 1D network **3e** in which 4,4′-dipyridyl-*N,N'*-dioxide (**1e**) alternate with 1,4-diiodotetrafluorobenzene (**2b**) is described. Single crystal X-ray analyses of **3e** shows how the oxygen atoms of the dioxide derivative **1e** work as effective electron donor sites and the iodine atoms of diiodoarene **2b** are the acceptor sites. To the best of our knowledge, the intermolecular O···I–C contact here observed is the shortest reported in the crystallographic literature. Other examples of PFC–HC complex formation starting from *N*-oxide derivatives are described, and co-crystallisation of diiodoarene **2b** in the presence of both nitrogen heteroaromatics and corresponding *N*-oxides have

[☆] Perfluorocarbon–hydrocarbon self assembly: part 15. For part 14, see Ref. 1.

Keywords: donor–acceptor interactions; iodine; halogen bonding; perfluorocarbon compounds; supramolecular chemistry.

* Corresponding authors. Tel.: +39-02-23993032; fax: +39-02-23993080; e-mail: giuseppe.resnati@polimi.it; pierangelo.metrangolo@polimi.it

Table 1. Upfield shifts of ^{19}F NMR signals of PFC iodides **2a,b** in the presence of oxygen and nitrogen donors **1a–d**

HC Donor	PFC Acceptor	HC/PFC molar ratio ^a	$\Delta\delta_{-\text{CF}_2-\text{I}/-\text{CF}=\text{C}-\text{I}}$ (ppm) ^b
Pyridine <i>N</i> -oxide (1a)	I–CF ₂ CF ₂ –I (2a)	1:1	0.42
Pyridine (1b)	I–CF ₂ CF ₂ –I (2a)	1:1	0.31
Pyridine <i>N</i> -oxide (1a)	I–CF ₂ CF ₂ –I (2a)	10:1	2.24
Pyridine (1b)	I–CF ₂ CF ₂ –I (2a)	10:1	2.11
4-Methylpyridine <i>N</i> -oxide (1c)	I–CF ₂ CF ₂ –I (2a)	1:1	0.52
4-Methylpyridine (1d)	I–CF ₂ CF ₂ –I (2a)	1:1	0.31
4-Methylpyridine <i>N</i> -oxide (1c)	I–CF ₂ CF ₂ –I (2a)	10:1	3.18
4-Methylpyridine (1d)	I–CF ₂ CF ₂ –I (2a)	10:1	2.46
Pyridine <i>N</i> -oxide (1a)	1,4-I ₂ –C ₆ F ₄ (2b)	1:1	0.10
Pyridine (1b)	1,4-I ₂ –C ₆ F ₄ (2b)	1:1	0.08
Pyridine <i>N</i> -oxide (1a)	1,4-I ₂ –C ₆ F ₄ (2b)	10:1	0.62
Pyridine (1b)	1,4-I ₂ –C ₆ F ₄ (2b)	10:1	0.54
4-Methylpyridine <i>N</i> -oxide (1c)	1,4-I ₂ –C ₆ F ₄ (2b)	1:1	0.13
4-Methylpyridine (1d)	1,4-I ₂ –C ₆ F ₄ (2b)	1:1	0.09
4-Methylpyridine <i>N</i> -oxide (1c)	1,4-I ₂ –C ₆ F ₄ (2b)	10:1	0.80
4-Methylpyridine (1d)	1,4-I ₂ –C ₆ F ₄ (2b)	10:1	0.54

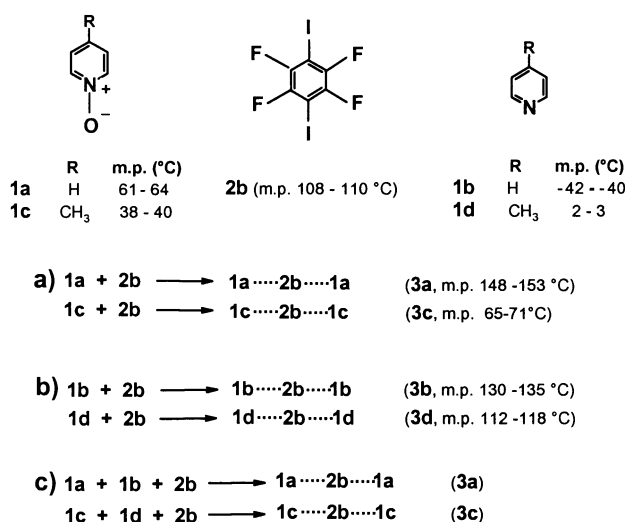
^a In all experiments PFC iodide **2** concentration was 0.19 M.

^b All spectra have been registered in CDCl₃; $\delta_{\text{ICF}_2\text{CF}_2\text{I}} = -53.20$ ppm, $\delta_{1,4\text{-I}_2\text{-C}_6\text{F}_4} = -118.55$ ppm.

established the oxygen versus nitrogen effectiveness in driving intermolecular recognition processes.

2. Results and discussion

The search for heteroatomic sites which can work as better electron donors than amine and pyridine moieties led us to also test sulphur and oxygen substituted HC modules. The most effective and simple tool to detect the formation of the halogen bonding in the liquid phase has been proven to be the ^{19}F NMR spectroscopy of PFC halides.⁹ In fact, on addition of the electron donor, the $-\text{CF}_2-\text{X}$ signal of perfluoroalkyl iodides, or bromides, and the $-\text{CF}=\text{C}-\text{X}$ signal of perfluoroaryl iodides, or bromides, shifts upfield.

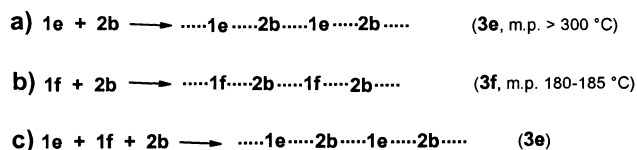
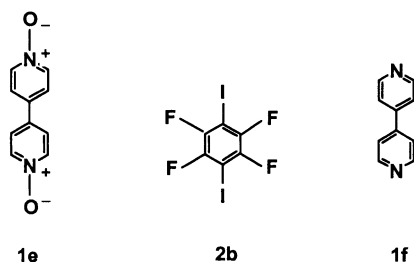


Scheme 1. Schematic diagram representing the formation of halogen bonded trimers: (a) formation of trimers **3a,c** containing pyridine *N*-oxide and 4-methylpyridine *N*-oxide (**1a,c** respectively) and 1,4-diiodo-tetrafluorobenzene (**2b**); (b) formation of trimers **3b,d** containing pyridine and 4-methylpyridine (**1b,d**) and 1,4-diiidotetrafluorobenzene (**2b**); (c) when the corresponding oxygen and nitrogen electron donors are present in the same solution together with the diiodoarene **2b**, the crystal containing the *N*-oxide forms preferentially as the O···I interaction prevails over the N···I interaction in identifying the modules to be involved in the co-crystal.

The shift value ($\Delta\delta_{-\text{CF}_2\text{X}/-\text{CF}=\text{C}-\text{X}}$ obtained as the difference between the chemical shift of the pure PFC halide and its chemical shift of the PFC halide in the presence of the electron donor module) increases on increasing the donor/acceptor ratio or the absolute concentration of the donor and acceptor in solution, consistent with a donor–acceptor association equilibrium in the liquid phase.

The $\Delta\delta_{-\text{CF}_2\text{X}/-\text{CF}=\text{C}-\text{X}}$ values are a sensitive probe to rank not only the acceptor but also the donor motifs according to the strength of the halogen bonding they inherently form. Structurally different nitrogen moieties give larger upfield shifts of the $-\text{CF}_2\text{X}/-\text{CF}=\text{C}-\text{X}$ signals than the corresponding oxygen moieties, for instance pyridines induce larger shifts than furans, tertiary amines than ethers, secondary and primary amines than alcohols.⁹ The basicity scale found via ^{19}F NMR spectroscopy strictly paralleled that obtained by using other analytical techniques, such as vibrational spectroscopies (through the blue and the red shifts induced by the halogen bonding on the basic and acid module vibrations, respectively).¹⁰ Other experimental proofs of the low ability of neutral oxygen atoms to behave as electron donor moieties towards mono- or dihalo-PFCs came from the structures of the co-crystals formed by HC modules containing both amine and ether donor sites.¹¹ In all these complexes, nitrogen and not oxygen atoms are involved into halogen bonding as is the case, for instance, of the two nitrogen atoms with respect to the six oxygen atoms present in Kryprofix[®] 2.2.2. (4,7,13,16,21,24-hexa-oxa-1,10-diazabicyclo[8.8.8]hexacosane).

Nevertheless the observation that the $\Delta\delta_{-\text{CF}_2\text{X}}$ shown by the ^{19}F NMR spectra of 1,2-diiidotetrafluoroethane in the presence of acetone, dimethylsulfoxide, and hexamethylphosphoramide were 3.63, 7.22, and 8.23,⁹ respectively, made us quite confident that for oxygen donors, the higher the electron density on the oxygen, the stronger is its electron donor ability towards R_F–X derivatives. For this reason we turned our attention on pyridine *N*-oxide derivatives. According to the charge-transfer theory¹² the extra negative charge on the oxygen atom should make it a better electron donor site and in fact the thermodynamic data for the formation of nitrogen heteroaromatic *N*-oxide/I₂



Scheme 2. Schematic diagram representing the formation of halogen bonded infinite chains: (a) formation of the infinite chain **3e** containing 4,4'-dipyridyl-*N,N'*-dioxide (**1e**) and 1,4-diiodotetrafluorobenzene (**2b**); (b) formation of the infinite chain **3f** containing 4,4'-dipyridyl (**1f**) and 1,4-diiodotetrafluorobenzene (**2b**); (c) when the three components are present at the same time in the solution the crystal containing the *N,N'*-dioxide preferentially forms as the O⋯I interaction prevails over the N⋯I interaction in identifying the modules to be involved in the co-crystal.

complexes¹³ indicate that the iodine complexing ability of *N*-oxides is stronger than for most oxygen donor moieties, alcohols, ethers, and ketones included.

In the presence of pyridine *N*-oxide (**1a**) and 4-methylpyridine *N*-oxide (**1c**) the ¹⁹F NMR signals of 1,2-diiodotetrafluoroethane (**2a**) and 1,4-diiodotetrafluorobenzene (**2b**) consistently shift upfield. The observed $\Delta\delta_F$ values (Table 1) increase with the electron donor concentration and are slightly larger than those given by pyridine and 4-methylpyridine (**1b** and **1d**, respectively) which are known to work as good donors.^{1,7} Clearly, in the liquid phase the *N*-oxide oxygen atom is a stronger donor than the nitrogen atoms in parent heteroaromatics.¹⁴

It is thus not surprising that when concentrated chloroform solutions of pyridine *N*-oxide **1a**, or 4-methylpyridine *N*-oxide **1c**, and diiodide **2b** are mixed at room temperature, the precipitation of the halogen bonded adducts **3a**, or **3c**,

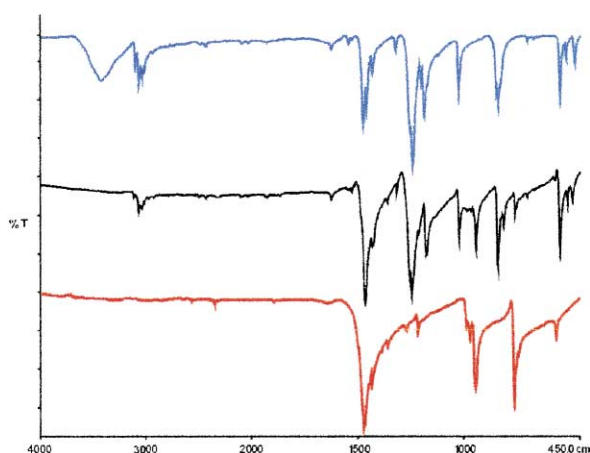


Figure 1. IR spectra (KBr, 4000–450 cm^{-1}) of polyhydrated, 4,4'-dipyridyl *N,N'*-dioxide (**1e**, blue), 1,4-diiodotetrafluorobenzene (**2b**, red), and the 1D infinite network they form (**3e**, black).

respectively, occurs immediately (Scheme 1) while starting from pyridine (**1b**), or 4-methylpyridine (**1d**), and the same diiodide **2b**, the solid trimers **3b** or **3d**, respectively, form only on nearly complete evaporation of the solvent. Interestingly, adducts **3a,c** show melting points which are higher than those of the starting components (e.g. mp_s of **1a**, **2b**, and **3a** are 61–64, 108–110, and 148–153°C, respectively) consistent with the formation of well defined intermolecular aggregates.

Compared to single modules **1** and **2**, IR spectra of adducts **3** show the band shifts and the band intensity variations typical for the presence of the halogen bonding.¹⁰ The $C_{\text{sp}^2}\text{-H}$ stretching modes of hydrocarbon modules **1a–d** (3020–3120 cm^{-1} region) undergo a blueshift¹⁵ and an intensity decrease on formation of both oxygen and nitrogen centred adducts **3a,c** and **3b,d**, respectively. Both changes are consistent with a higher positive charge on hydrogen atoms as a result of an $n \rightarrow \sigma^*$ electron donation from oxygen, or nitrogen, to iodine. The intermolecular interaction also affects the vibrations of the perfluorocarbon module **2b** (e.g. absorptions at 1468 and 564 cm^{-1}) and once again the shifts caused by oxygen and nitrogen donors are in the same direction.

In order to directly compare the oxygen versus nitrogen ability in driving the intermolecular recognition process, a chloroform solution of the diiodide **2b** was added to a chloroform solution containing equimolar amounts of pyridine (**1b**) and its *N*-oxide **1a**. The complex **3a** containing the latter donor precipitates in a pure form and the parent heterocycle **1b** remains in solution (as confirmed through microanalysis, TLC and NMR analyses of ¹H and ¹⁹F nuclei). Similarly, solvent evaporation from a solution containing equimolar amounts of **1c**, **1d**, and **2b** preferentially affords the solid complex **3c**, in both competitive co-crystal formations the oxygen donor proving more effective than the nitrogen donor in controlling the construction of PFC–HC supramolecular architecture.

A quite similar behaviour was also shown by 4,4'-dipyridyl *N,N'*-dioxide (**1e**) and 4,4'-dipyridine (**1f**). When the two compounds were separately challenged with the diiodo-perfluoroarene **2b** the 1D infinite chains **3e** and **3f**, where the oxygen and nitrogen atoms are halogen bonded to the iodine atoms, are formed as white and crystalline solids which are stable at room temperature and in the air (Scheme 2). In order to directly contrast the O⋯I–C and the N⋯I–C interactions, a competitive experiment was once again performed. Equimolar amounts of the oxygen and nitrogen substituted donors, **1e** and **1f**, respectively, and of the diiodoarene **2b** were dissolved in chloroform/methanol. Evaporation of the solvent afforded the *N*-oxide containing co-polymer **3e** and the parent dipyridine **1f** remained in solution. In this case too the O⋯I–C interaction dominates over the N⋯I–C interaction and singles out the molecules that will be involved in the construction of the supramolecular architecture. Moreover, nitrogen atoms of pyridine derivatives¹⁶ and oxygen atoms of corresponding *N*-oxides¹⁷ are quite prone to hydrogen bonding and under the crystallisation conditions they are bound to the hydrogen atoms of methanol and water (the commercial polyhydrated dioxide **1e** was used as starting material). Therefore, the

Table 2. Details of data collection and of structure refinement for **3e** and **3f**

Compound	3e	3f
Formula	C ₁₀ H ₈ N ₂ O ₂ ·C ₆ F ₄ I ₂	C ₁₀ H ₈ N ₂ ·C ₆ F ₄ I ₂
<i>M_r</i>	590.04	558.04
Crystal dimensions (mm ³)	0.36×0.20×0.11	0.34×0.25×0.20
System, space group	Triclinic, <i>P</i> 1	Monoclinic, <i>P</i> 2 ₁ / <i>c</i>
<i>a</i> (Å)	4.2954(4)	8.3617(9)
<i>b</i> (Å)	8.1290(8)	5.7270(6)
<i>c</i> (Å)	13.6474(14)	17.7928(16)
α (°)	100.732(8)	90
β (°)	98.823(8)	96.266(9)
γ (°)	103.792(8)	90
<i>V</i> (Å ³)	444.82(8)	846.96(15)
<i>Z</i> , <i>D_c</i> (gcm ⁻³), μ (MoK α) (mm ⁻¹)	1, 2.202, 3.587	2, 2.188, 3.753
N. Refl. collected, independent, observed [<i>I</i> > 2 σ (<i>I</i>)]	2883, 2568, 2333	4991, 2464, 2072
<i>R_{ave}</i>	0.0190	0.0198
Refined parameters, goodness-of-fit	130, 1.041	122, 1.027
<i>R</i> (<i>F</i>) on all reflections,	0.0330, 0.0296	0.0370, 0.0287
<i>R</i> (<i>F</i>) on observed		
<i>wR</i> (<i>F</i> ²) on all reflections,	0.0843, 0.0816	0.0702, 0.0673
<i>wR</i> (<i>F</i> ²) on observed		
$\Delta\rho_{\min}$, $\Delta\rho_{\max}$ e(Å ⁻³)	-0.40, 0.78	-0.78, 0.77

O··I–C halogen bonding dominates not only over the N··I–C interaction but also over the O··H–O and the N··H–O hydrogen bonding in controlling self-assembly processes.

The 1:1 ratio of the HC and PFC modules in **3e,f** was established through microanalyses and ¹H/¹⁹F NMR spectra in the presence of (CF₃CH₂)₂O as internal standard. The changes in IR absorptions of both donor and acceptor modules **1e,f** and **2b** when giving rise to infinite chains **3e,f** strictly parallel those described above for **3a–d** for-

mation. It is particularly interesting that comparing the IR spectrum of starting 4,4'-dipyridyl *N,N'*-dioxide (**1e**) with that of the halogen-bonded adduct **3e**, the absorption related to the hydrogen-bonded crystallisation water in **1e** was completely missing (Fig. 1), this being largely independent from the solvent used for the crystallisation. This peculiar property of halogen bonded PFC iodides to substitute water in the crystal packing of the lone-pair donors, coupled with the high volatility of PFC derivatives which allows their easy removal from the halogen bonded co-crystal, could be developed as a general, low cost, and large scale way to obtain hygroscopic organic compounds in anhydrous form.

The structural details of the supramolecular architectures **3e,f** were established through single crystal X-ray analyses (Table 2, Figs. 2 and 3). Some similarities exist between the two crystal packings and pertain to the pattern of intermolecular interactions while the main differences pertain to the relative arrangement of the aromatic rings of PFC and HC modules.

Specifically, the O··I–C and the N··I–C distances are 2.754(2) and 2.864(2) Å, respectively, both being significantly shorter than the sum of van der Waals radii. For **3e** this shortening is 22.4 or 21.3% if Pauling's¹⁸ or Bondi's¹⁹ radii are used, respectively, and the corresponding values for **3f** are 19.3 and 18.9%. Irrespective of the database used for the van der Waals radii, the shortening of the distance between the halogen bonded nuclei is greater when oxygen than nitrogen is involved, once again consistent with oxygen being a better electron donor than nitrogen in these systems. It is really interesting to observe that a careful survey of the crystallographic literature (Cambridge Structural Database, CSD, version 5.1.10, 1 October 2000,

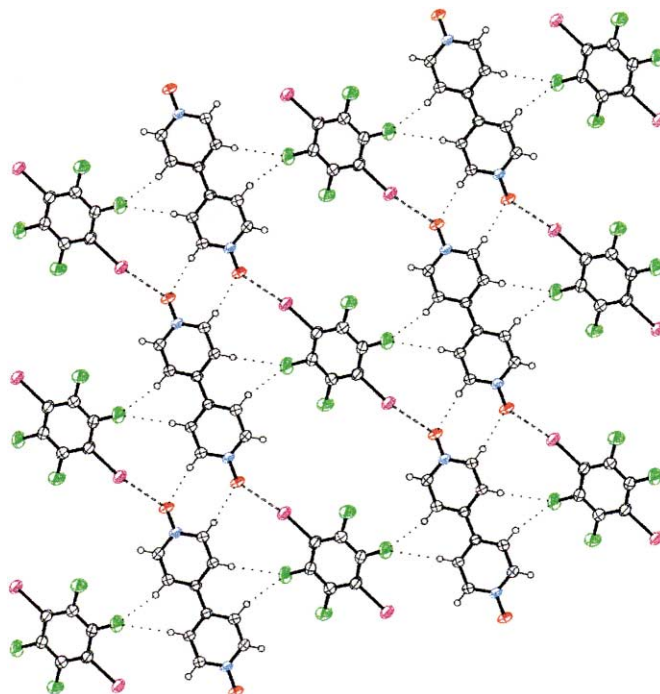


Figure 2. Crystal packing of **3e** in the plane containing most of the intermolecular interactions. The strong halogen bondings are dashed, the weak hydrogen bondings are dotted. Colours are as follows: violet, iodine; red, oxygen; blue, nitrogen; green, fluorine; black, carbon and hydrogen.

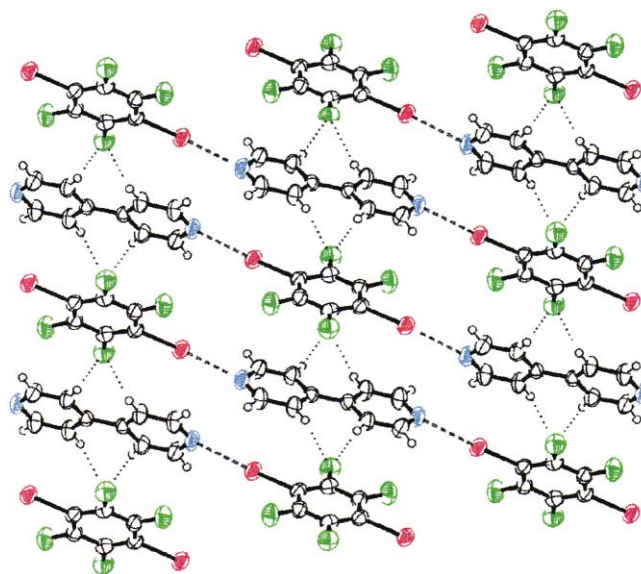


Figure 3. Crystal packing of **3f** viewed down the *b*-axis. The strong halogen bondings are dashed, the weak hydrogen bondings are dotted. Colours are as follows: violet, iodine; blue, nitrogen; green, fluorine; black, carbon and hydrogen.

22,400 crystal structures having atomic co-ordinates available) revealed that the C–I···O distance observed in **3e** is significantly shorter than that found in all other reported related crystals (Fig. 4), a further proof of the strength of the interaction. The O···I–C angle is 170.31(11)° when the N···I–C angle is 177.3(3)°³¹ this nearly linear arrangement being consistent with the n→σ* character of the halogen bonding.⁴

Both in **3e** and in **3f** the non-covalent and halogen bonded chains are cross linked by interactions other than the halogen bonding. In **3e** the *N*-oxide oxygen gives a short

O···H–C contact to the *ortho* hydrogen of the dipyridyl module of a nearby chain²⁰ (O···H5_{-2-x,-1-y,-z} 2.32(4) Å) and two fluorine atoms of any diiodoarene module give weak C–F···H–C interactions^{7g,21} with two *meta* hydrogens of the dipyridyl modules of different chains (F···H2_{x,y,1+z} 2.65(4) Å). Slightly corrugated planes are thus formed which are connected to each other by fluorine–hydrogen contacts (F2···H1_{+x,y,1+z} 2.67(5) Å) and by π–π interactions involving dipyridyl modules (interplanar distance 3.414(2) Å, the interplanar distance between PFC modules being slightly larger, 3.662(2) Å). In **3f**, short fluorine–hydrogen contacts exist between two 1,4 positioned fluorine atoms of the diiodoarene modules **2b** and two *meta* hydrogens of adjacent dipyridyl modules **1f** (F1···H2_{1-x,1/2+y,1/2-z} 2.64(3) Å and F1···H4_{x,3/2-y,1/2+z} 2.63(3) Å).

As far as packing differences between **3e** and **3f** are concerned, in **3e** all the halogen bonded chains are parallel with each other while in **3f** they are exchanged through a 2₁ axis and the formed angle is approximately 17°. Moreover, the π–π interactions in **3f** are between pyridine and diiodoarene rings which form columns where the angle between the mean planes of the two molecules is 6.01(10)° and the mean interplanar distance is 3.525(15) Å. Both in **3e** and in **3f** the two rings of dipyridyl *N,N'*-dioxide and of dipyridine are perfectly coplanar (the two modules lay on a centre of symmetry) and the diiodoarene module is tilted, the angles between the mean planes being 16.7(2) and 61.00(9)°, respectively.

3. Conclusion

Towards PFC-iodides, used as electron acceptor motifs, HC-ethers and -alcohols behave as poor electron donor motifs,^{9,11} while it is shown here how HC-heteroaromatic *N*-oxide work as quite effective donors both in the liquid and in the solid phase. This indicates that not only nitrogen but also oxygen containing donors may provide excellent arrays

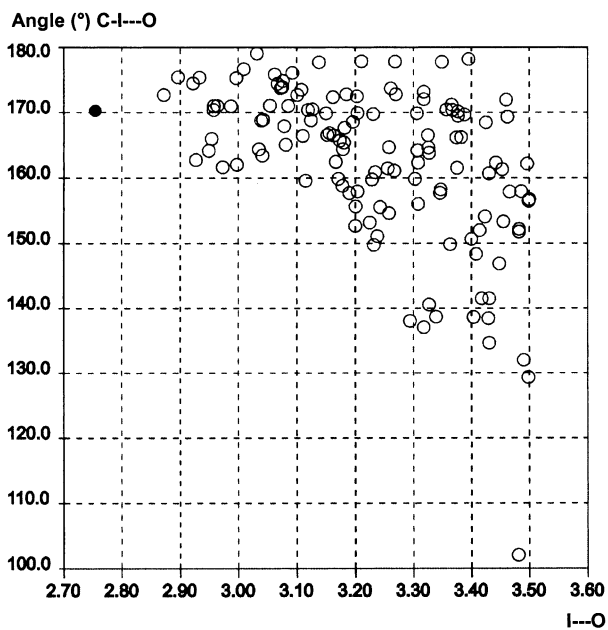


Figure 4. Scatterplot of C–I···O angles versus O···I distances for intermolecular C–I···O interactions. Only error free and non-polymeric structures showing no disorder and with *R* < 0.06 are reported. Compound **3e** is the black dot.

for the self-assembly of PFC and HC derivatives. ^{19}F NMR analyses and competitive co-crystallisation experiments show that, as far as halogen bonding formation is concerned, *N*-oxides are superior to their parent heteroaryls. A further indication of the strength of the $\text{R}_\text{F}\cdots\text{I}\cdots\text{O}$ interaction here discussed is that the $\text{C}\cdots\text{I}\cdots\text{O}$ distance observed in the infinite chain formed by 4,4'-dipyridyl *N,N'*-dioxide (**1e**) with 1,4-diiodotetrafluorobenzene (**2b**) is the shortest one reported to date in the crystallographic literature. It is interesting to observe that the previous minimum for the $\text{C}\cdots\text{I}\cdots\text{O}$ interaction was observed in 1-(2-deoxy-2-fluoro- α -D-arabinopyranosyl)-5-iodouracil²² and the crystal structure of the thyroxine–prealbumin complex showed a close contact between one of thyroxine iodines and the carbonyl oxygen of Ala-109A in the prealbumin backbone ($\text{C}\cdots\text{I}\cdots\text{O}$ 2.96 Å, $\text{C}\cdots\text{I}\cdots\text{O}$ 161°).²³ The relevance of the $\text{C}\cdots\text{I}\cdots\text{O}$ interaction extends therefore to bioactive compounds and substrate–protein binding.

The pyridine motif has already allowed a wide diversity of PFC–HC supramolecular architectures to be formed^{1,3i,7} and corresponding *N*-oxides may thus have an enormous potential for the construction of PFC incorporating networks. Indeed, it is well known how *N*-oxides can form $\text{N}\cdots\text{O}\cdots\text{X}$ non-covalent interactions where the electron acceptor motif X is an hydrogen atom (hydrogen bonding)^{17,24} or a metal ion (metal coordination).²⁵ For instance, bis-*N*-oxides afforded lanthanide cation ligands superior in many respects (complex strength, pH sensitivity, luminescence) to their parent biheteroaryls²⁶ and they have been recently used to construct inorganic networks also with d-block elements.²⁷ The relevance of heteroaromatic *N*-oxides in crystal engineering is here extended to $\text{N}\cdots\text{O}\cdots\text{X}$ adducts where X is an iodine atom (halogen bonding). The highly localised negative charge on the oxygen atom of *N*-oxides is probably responsible for their effectiveness in $\text{N}\cdots\text{O}\cdots\text{X}$ non-covalent interaction formation. The negative charge localized on the oxygen atom is greater in aliphatic *N*-oxides than in heteroaromatic analogues and our current work seeks to investigate if this enables aliphatic *N*-oxides to form halogen bondings even shorter than those reported here.

4. Experimental

4.1. General methods

All materials were obtained from commercial suppliers and were used without further purification. ^1H - and ^{19}F NMR spectra were recorded with a Bruker AV 500 spectrometer; tetramethylsilane and CFCl_3 were used as internal standards, respectively. IR Spectra were recorded with a Perkin–Elmer 2000 FT-IR spectrophotometer. Selected IR and $^1\text{H}/^{19}\text{F}$ NMR spectral properties of starting modules are reported to show the changes occurring on PFC–HC adduct formation. Elemental analyses were performed by Redox Snc, Cologno Monzese, Milan, Italy. Differences between calculated values and those found are strictly related to the difficulties to obtain good elemental analyses of mixed perfluorocarbon–hydrocarbon compounds. X-ray crystal structure was determined using a Bruker P4 diffractometer.

4.1.1. General procedure. Formation of non covalent co-polymer **3e** compounded by 4,4'-dipyridyl *N,N'*-dioxide (**1e**) and 1,4-diiodotetrafluorobenzene (**2b**).

At room temperature, a solution of the diiodoarene **2b** (1.24 g, 3.09 mmol) in chloroform/methanol (95:5 ratio, 2.5 mL) was added to a 10 mL clear borosilicate vial containing a solution of dipyridyl-dioxide **1e** (polyhydrate sample, Aldrich, 690 mg) in chloroform/methanol (70:30 ratio, 4.5 mL). The open vial was placed in a closed cylindrical wide-mouth bottle (50 mL) containing vaseline oil. Volatile solvents were allowed to diffuse at room temperature and after 6 h the non covalent co-polymer **3e** was filtered (1.21 g) as a white crystalline solid and washed with cold dichloromethane $\text{mp} > 300^\circ\text{C}$, elemental analyses: (%): Calc. For $\text{C}_{16}\text{H}_8\text{F}_4\text{I}_2\text{N}_2\text{O}_2$: C 32.54; H 1.35; I 43.05; N 4.74; found: C 32.18; H 1.88; I 43.75; N 4.68. ^{19}F NMR: Pure 1,4-diiodotetrafluorobenzene (**2b**) (0.16 M, $\text{CDCl}_3/\text{CD}_3\text{OD}$ 4:1): $\delta_\text{F} = -118.85$; co-crystal **3e**: $\Delta\delta_\text{F} = \delta_\text{pure } 2\text{b} - \delta_{3\text{e}}$ (0.16 M) = 0.05. ^1H NMR: Pure polyhydrated 4,4'-dipyridyl *N,N'*-dioxide (**1e**, Aldrich) (0.08 M in $\text{CDCl}_3/\text{CD}_3\text{OD}$ 4:1): $\delta_\text{H} = 7.74$ ($\text{CH}=\text{CH}=\text{N}$), 8.35 ($\text{CH}=\text{N}$); co-crystal **3e**: $\Delta\delta_\text{H} = \delta_\text{pure polyhydrated } 1\text{e} - \delta_{(3\text{e})}$ (0.08 M, $\text{CDCl}_3/\text{CD}_3\text{OD}$ 4:1) = -0.04 ($\text{CH}=\text{CH}=\text{N}$), -0.03 ($\text{CH}=\text{N}$). In another experiment ^1H - and ^{19}F NMR spectra were registered in the presence of 2,2,2-trifluoroethyl ether as an internal standard. On calibrating integration parameters so that in the ^1H NMR spectrum the CH_2O quartet of 2,2,2-trifluoroethyl ether was corresponding to four and in the ^{19}F NMR spectrum the CF_3 triplet of 2,2,2-trifluoroethyl ether was corresponding to six, the ratio of the $-\text{CF}=\text{CI}$ signal area (deriving from **2b**) and the $\text{CH}=\text{N}$ signal area (deriving from **1e**) is 1:1 thus revealing that the **1e:2b** ratio in **3e** is 1:1. IR (KBr pellets, selected bands): Pure 1,4-diiodotetrafluorobenzene (**2b**): 1468, 1241, 944, 760, 564 cm^{-1} ; pure polyhydrated 4,4'-dipyridyl *N,N'*-dioxide (**1e**, Aldrich): 3067, 3037, 1241, 1187, 548, 510, 478 cm^{-1} ; co-crystal **3e**: 3070, 3040, 1244, 1179, 1465, 1179, 944, 759, 572, 547, 511, 488 cm^{-1} .

4.1.2. Non covalent co-polymer **3f** compounded by 4,4'-dipyridyl (**1f**) and 1,4-diiodotetrafluorobenzene (**2b**).

Dipyridyl **1f** (420 mg, 2.69 mmol) and diiodoarene **2b** (1.08 g, 2.69 mmol) were co-crystallised from acetone/vaseline oil through the diffusion technique described above to give the non covalent co-polymer **3f** (1.22 g, mp 180–185°C). Elemental analyses: (%): Calc. For $\text{C}_{16}\text{H}_8\text{F}_4\text{I}_2\text{N}_2$: C 34.41; H 1.43; I 45.52; N 5.02; found: C 34.06; H 1.85; I 46.21; N 4.97. The 1:1 ratio of **1f** and **2b** in **3f** was confirmed through $^1\text{H}/^{19}\text{F}$ NMR analyses in the presence of 2,2,2-trifluoroethyl ether (see above). ^{19}F NMR: Pure 1,4-diiodotetrafluorobenzene (**2b**) (0.16 M, CDCl_3): $\delta_\text{F} = -118.55$; co-crystal **3f**: $\Delta\delta_\text{F} = \delta_\text{pure } 2\text{b} - \delta_{3\text{f}}$ (0.16 M, CDCl_3) = 0.04. ^1H NMR: Pure 4,4'-dipyridyl (**1f**) (0.18 M, CDCl_3): $\delta_\text{H} = 8.75$ ($\text{CH}=\text{CH}=\text{N}$), 7.55 ($\text{CH}=\text{N}$); co-crystal **3f**: $\Delta\delta_\text{H} = \delta_\text{pure } 1\text{f} - \delta_{3\text{f}}$ (0.18 M, CDCl_3) = -0.01 ($\text{CH}=\text{CH}=\text{N}$), -0.01 ($\text{CH}=\text{N}$). IR (KBr pellets, selected bands): pure 4,4'-dipyridyl (**1f**): 3026, 807, 608, 570 cm^{-1} ; co-crystal **3f**: 3028, 1458, 938, 757, 802, 613, 575 cm^{-1} .

4.1.3. Trimer **3a** compounded by pyridine *N*-oxide (**1a**) and 1,4-diiodotetrafluorobenzene (**2b**).

Pyridine *N*-oxide (**1a**, 238 mg, 2.5 mmol) and diiodoarene **2b** (502 mg, 1.25 mmol) were crystallised from chloroform/vaseline oil

through the diffusion technique described above to give the non covalent trimer **3a** (608 mg, mp 148–153°C). Elemental analyses: (%): Calc. for C₁₆H₁₀F₄I₂N₂O₂: C 32.43; H 1.69; I 42.90; N 4.73; found: C 31.96; H 1.96; I 43.23; N 5.85. The 2:1 ratio of **1a** and **2b** in **3a** was confirmed through ¹H/¹⁹F NMR analyses in the presence of 2,2,2-trifluoroethyl ether (see above). ¹⁹F NMR: see Table 1. IR (KBr pellets, selected bands): pure pyridine *N*-oxide **1a**: 3110, 1234, 549, 512, 469 cm⁻¹; co-crystal **3a**: 3116, 1464, 1220, 942, 758, 573, 548, 504, 480 cm⁻¹.

4.1.4. Trimer 3b compounded by pyridine (1b) and 1,4-diiodotetrafluorobenzene (2b). Pyridine (**1b**, 2.5 mmol) and diiodoarene (**2b**, 1.25 mmol) were co-crystallised from acetone/vaseline oil through the diffusion technique described above to give the non covalent trimer **3b** (635 mg, mp 130–135°C). Elemental analyses: (%): Calc. for C₁₆H₁₀F₄I₂N₂: C 34.29; H 1.78; I 43.35; N 5.00; found: C 33.86; H 2.03; I 43.71; N 5.11. The 2:1 ratio of **1b** and **2b** in **3b** was confirmed through ¹H/¹⁹F NMR analyses in the presence of 2,2,2-trifluoroethyl ether (see above). ¹⁹F NMR: see Table 1. IR (KBr pellets, selected bands): pure pyridine **1b**: 3027, 1582, 991, 704 cm⁻¹; co-crystal **3b**: 3036, 1587, 998, 701, 1464, 944, 700, 564 cm⁻¹.

4.1.5. Trimer 3c compounded by 4-methylpyridine N-oxide (1c) and 1,4-diiodotetrafluorobenzene (2b). 4-Methylpyridine *N*-oxide (**1c**, 2.5 mmol) and diiodoarene **2b** (1.25 mmol) were co-crystallised from chloroform/vaseline oil through the diffusion technique described above to give the non covalent trimer **3c** (659 mg, mp 65–71°C). Elemental analyses: (%): Calc. for C₁₈H₁₄F₄I₂N₂O₂: C 34.84; H 2.26; I 40.96; N 4.52; found: C 34.53; H 2.45; I 41.37; N 4.81. The 2:1 ratio of **1c** and **2b** in **3c** was confirmed through ¹H/¹⁹F NMR analyses in the presence of 2,2,2-trifluoroethyl ether (see above). ¹⁹F NMR: see Table 1. IR (KBr pellets, selected bands): pure 4-methylpyridine *N*-oxide **1c**: 3092, 3057, 1252, 1191, 524, 482 cm⁻¹; co-crystal **3c**: 3110, 3089, 1211, 1177, 515, 475 cm⁻¹.

4.1.6. Trimer 3d compounded by 4-methylpyridine (1d) and 1,4-diiodotetrafluorobenzene (2b). 4-Methylpyridine *N*-oxide (**1d**, 2.5 mmol) and diiodoarene **2b** (1.25 mmol) were co-crystallised from acetone/vaseline oil through the diffusion technique described above to give the non covalent trimer **3d** (633 mg, mp 112–118°C). Elemental analyses: (%): Calc. for C₁₈H₁₄F₄I₂N₂: C 36.73; H 2.38; I 43.20; N 4.76; found: C 36.40; H 2.54; I 43.59; N 5.04. The 2:1 ratio of **1a** and **2b** in **3a** was confirmed through ¹H/¹⁹F NMR analyses in the presence of 2,2,2-trifluoroethyl ether (see above). ¹⁹F NMR: see Table 1. IR (KBr pellets, selected bands): pure 4-methylpyridine *N*-oxide **1d**: 3030, 1607, 802, 486 cm⁻¹; co-crystal **3d**: 3038, 1608, 1457, 940, 795, 761, 572, 483 cm⁻¹.

4.2. X-Ray crystallographic study of 3e and 3f

Single crystal data of **3e** and **3f** were collected on a Bruker P4 diffractometer with graphite monochromatized MoK α radiation ($\lambda=0.71073$ Å). Absorption correction was based on Ψ -scans.²⁸ The structures were solved by SIR-92,²⁹ and refined on *F*² by SHELX-97.³⁰ Details of data

collection and refinement are reported in Table 2. Crystallographic data (excluding structure factors) for the structures in this paper have been deposited with the Cambridge Crystallographic Data Centre as supplementary publication number CCDC 163294 (**3e**) and 163295 (**3f**). Copies of the data can be obtained, free of charge on application to CCDC, 12 union Road, Cambridge CB2 1EZ, UK [fax: (+44) 1223-336-033 or e-mail: deposit@ccdc.cam.ac.uk].

Acknowledgements

This work was supported by Murst (Cofinanziamento 1999) and the European Union (COST Networks D12-0012 and RTN Network HPRN-CT-2000-00002).

References

- Part 14: Metrangolo, P.; Resnati, G. *Chem. Eur. J.* **2001**, *7*, 2511–2519.
- (a) Hassel, O. *Science* **1970**, *170*, 497–502. (b) Dumas, J. M.; Gomel, L.; Guerin, M. In *The Chemistry of Functional Groups, Supplement D*; Patai, S., Rappoport, Z., Eds.; Wiley: New York, 1983. (c) Bent, H. A. *Chem. Rev.* **1968**, *68*, 587–648.
- (a) Thaimattam, R.; Sharma, C. V. K.; Clearfield, A.; Desiraju, G. R. *Cryst. Growth Des.* **2001**, *1*, 103–106. (b) Pedireddi, V. R.; Ranganathan, A. *Tetrahedron Lett.* **1998**, *39*, 1803–1806. (c) Weiss, R.; Schwab, O.; Hampel, F. *Chem. Eur. J.* **1999**, *5*, 968–974. (d) Imakubo, T.; Maruyama, T.; Sawa, H.; Kobayashi, K. *Chem. Commun.* **1998**, 2021–2022. (e) Imakubo, T.; Sawa, H.; Kato, R. *Chem. Commun.* **1995**, 1667–1668. (f) Hulliger, J.; Langley, P. J. *Chem. Commun.* **1998**, 2557–2558. (g) Masciocchi, N.; Bergamo, M.; Sironi, A. *Chem. Commun.* **1998**, 1347–1348. (h) Weiss, R.; Reching, M.; Hampel, F.; Wolski, A. *Angew. Chem., Int. Ed. Engl.* **1995**, *34*, 441–443. (i) Walsh, R. B.; Padgett, C. W.; Metrangolo, P.; Resnati, G.; Hanks, T. W.; Pennington, W. T. *Cryst. Growth Des.* **2001**, *1*, 165–175. (j) Allen, F. H.; Biradha, K.; Desiraju, G. R.; Hoy, V. J.; Howard, J. A. K.; Sarma, J. A. R. P.; Thaimattam, R. *Chem. Commun.* **1997**, 101–102.
- Foster, R. *Organic Charge-Transfer Complexes*; Academic: London, 1969; p 100.
- Valerio, G.; Raos, G.; Meille, S. V.; Metrangolo, P.; Resnati, G. *J. Phys. Chem. A* **2000**, *104*, 1617–1620.
- (a) Smart, B. E. In *Organofluorine Chemistry: Principles and Commercial Applications*; Banks, R. E., Smart, B. E., Tatlow, J. C., Eds.; Plenum: New York, 1994. (b) Hildebrand, J.; Cochran, D. R. F. *J. Am. Chem. Soc.* **1949**, *71*, 22–25. (c) Dorset, D. L. *Macromolecules* **1990**, *23*, 894901.
- (a) Lunghi, A.; Cardillo, P.; Messina, M. T.; Metrangolo, P.; Panzeri, W.; Resnati, G. *J. Fluorine Chem.* **1998**, *91*, 191–194. (b) Corradi, E.; Meille, S. V.; Messina, M. T.; Metrangolo, P.; Resnati, G. *Angew. Chem., Int. Ed. Engl.* **2000**, *39*, 1782–1786. (c) Corradi, E.; Meille, S. V.; Messina, M. T.; Metrangolo, P.; Resnati, G. *Tetrahedron Lett.* **1999**, *40*, 7519–7523. (d) Messina, M. T.; Metrangolo, P.; Pappalardo, S.; Parisi, M. F.; Pilati, T.; Resnati, G. *Chem. Eur. J.* **2000**, *6*, 3495–3500. (e) Messina, M. T.; Metrangolo, P.; Resnati, G. *Asymmetric Fluoroorganic Chemistry: Synthesis, Applications*

- and Future Directions; ACS Symposium Series No. 746, ACS: Washington, DC, 1999. (f) Manfredi, A.; Messina, M. T.; Metrangolo, P.; Pilati, T.; Quici, S.; Resnati, G. *Supramol. Chem.* **2000**, *12*, 405–410. (g) Metrangolo, P.; Panzeri, W.; Resnati, G.; Forni, A.; Pilati, T.; Fontana, F. *Supramol. Chem.* **2001**, in press.
- Pilati, T.; Metrangolo, P.; Resnati, G. Unpublished results.
 - Metrangolo, P.; Panzeri, W.; Ragg, E.; Resnati, G. *Tetrahedron Lett.* **1998**, *39*, 9069–9072.
 - Messina, M. T.; Metrangolo, P.; Navarrini, W.; Radice, S.; Resnati, G.; Zerbi, G. *J. Mol. Struct.* **2000**, *524*, 87–94.
 - (a) Amico, V.; Meille, S. V.; Corradi, E.; Messina, M. T.; Resnati, G. *J. Am. Chem. Soc.* **1998**, *120*, 8261–8262. (b) Messina, M. V.; Metrangolo, P.; Pilati, T.; Resnati, G. *New J. Chem.* **2000**, *24*, 777–780. (c) Cardillo, P.; Corradi, E.; Lunghi, A.; Meille, S. V.; Messina, M. T.; Metrangolo, P.; Resnati, G. *Tetrahedron* **2000**, *56*, 5535–5550.
 - (a) Mulliken, R. S. *J. Am. Chem. Soc.* **1952**, *74*, 811–824. (b) Mulliken, R. S. *J. Phys. Chem.* **1952**, *56*, 801–822. (c) Mulliken, R. S.; Person, W. B. *Ann. Rev. Phys. Chem.* **1962**, *13*, 107–126.
 - (a) Kubota, T. *J. Am. Chem. Soc.* **1965**, *87*, 458–468. (b) Kulevsky, N.; Severson, Jr., R. G. *J. Phys. Chem.* **1971**, *75*, 2504–2506.
 - Significant changes were also observed in the ^1H spectra of the HC donor molecules where low field shifts of the signals related to the protons *meta* to the nitrogen atom have been observed.
 - (a) Yada, H.; Tanaka, J.; Nagakura, S. *J. Mol. Spectrosc.* **1962**, *9*, 461–468. (b) VanPaasschen, J. M.; Geanangel, R. A. *Can. J. Chem.* **1975**, *53*, 723–726. (c) Gayles, J. N. *J. Chem. Phys.* **1968**, *49*, 1840–1847. (d) Zingaro, R. A.; Tolberg, W. E. *J. Am. Chem. Soc.* **1959**, *81*, 1353–1357. (e) Yokobayashi, K.; Watari, F.; Aida, K. *Spectrochim. Acta* **1968**, *24A*, 1651–1655.
 - Koyama, T.; Wakisaka, A. *J. Chem. Soc., Faraday Trans.* **1997**, *93*, 3813–3817.
 - Thaimattam, R.; Shekhar Reddy, D.; Xue, F.; Mak, T. C. W.; Nangia, A.; Desiraju, G. R. *J. Chem. Soc., Perkin Trans. 2* **1998**, 1783–1789.
 - Pauling, L. *The Nature of the Chemical Bond*; 3rd ed.; Cornell University: Ithaca, NY, 1960.
 - Bondi, A. *J. Phys. Chem.* **1964**, *68*, 441–451.
 - Similar C–H···O–N interactions cross link the infinite chains formed by **1e** and water in 1:2 co-crystals (Ref. 17) and have been observed to support *N*-oxide network formations: Bodige, S. G.; Rogers, R. D.; Blackstock, S. C. *Chem. Commun.* **1997**, 1669–1670.
 - Thalladi, V. R.; Weiss, H. C.; Bläser, D.; Boese, R.; Nangia, A.; Desiraju, G. R. *J. Am. Chem. Soc.* **1998**, *120*, 8702–8710.
 - De Winter, H. L.; Blaton, N. M.; Peeters, O. M.; De Ranter, C.; Van Aerschot, A.; Herdewijn, P. J. *Acta Crystallogr. C* **1991**, *47*, 2245–2247.
 - (a) Vivian, C.; Murray-Rust, P. *J. Mol. Struct.* **1984**, *112*, 189–200. (b) Lommerse, J. P. M.; Taylor, R. *J. Enzyme Inhib.* **1997**, *11*, 223–243. (c) Steinrauf, L. K.; Hamilton, J. A.; Braden, B. C.; Murrell, J. R.; Benson, M. D. *J. Biol. Chem.* **1993**, *268*, 2425–2430.
 - (a) Videnova-Adrabinaska, V.; Janeczko, E. *Chem. Commun.* **1999**, 1527–1528. (b) Kulevsky, N.; Lewis, L. *J. Phys. Chem.* **1972**, *76*, 3502–3503.
 - (a) Long, D.-L.; Blake, A. J.; Champness, R. N.; Schröder *Chem. Commun.* **2000**, 1369–1370. (b) Shupack, S. I.; Orchin, M. *J. Am. Chem. Soc.* **1964**, *86*, 586–590.
 - (a) Pietraszkiewicz, M.; Pappalardo, S.; Finocchiaro, P.; Mamo, A.; Karpiuk, J. *Chem. Commun.* **1989**, 1907–1908. (b) Lehen, J.-M.; Pietraszkiewicz, M.; Karpiuk, J. *Helv. Chim. Acta* **1990**, *73*, 106–111. (c) Lehn, J.-M.; Roth, C. O. *Helv. Chim. Acta* **1991**, *74*, 572–578. (d) Prodi, L.; Maestri, M.; Balzani, V.; Lehn, J.-M.; Roth, C. O. *Chem. Phys. Lett.* **1991**, *180*, 45–50. (e) Pietraszkiewicz, M.; Karpiuk, J.; Rout, A. K. *Pure Appl. Chem.* **1993**, *65*, 563–566.
 - Long, D.-L.; Blake, A. J.; Champness, R. N.; Schröder, M. *Chem. Commun.* **2001**, 2273–2274.
 - North, A. C. T.; Phillips, D. C.; Mathews, F. S. *Acta Crystallogr. A* **1968**, *24*, 435.
 - Altomare, A.; Cascarano, G.; Giacovazzo, G.; Guagliardi, A.; Burla, M. C.; Polidori, G.; Camalli, G. *J. Appl. Crystallogr.* **1994**, *27*, 435.
 - Sheldrick, G. M. *SHELX-97. Program for the Refinement of Crystal Structures*; University of Göttingen: Germany, 1997.